HHS Public Access

Author manuscript

Nat Med. Author manuscript; available in PMC 2018 March 29.

Published in final edited form as:

Nat Med. 2018 March ; 24(3): 360–367. doi:10.1038/nm.4477.

Antagonism of PPARγ signaling expands human hematopoietic stem and progenitor cells by enhancing glycolysis

Bin Guo[1,*], **Xinxin Huang**[1,*], **Man Ryul Lee**[2], **Sang A Lee**[2], and **Hal E. Broxmeyer**[1]

[1]Department of Microbiology and Immunology, Indiana University School of Medicine, Indianapolis, IN 46202, USA

[2]Soonchunhyang Institute of Medi-bio Science (SIMS), Soon Chun Hyang University, Cheonan-si, Chungcheongnam-do, Republic of Korea

Abstract

Hematopoietic stem cells (HSCs) quiescently reside in bone marrow niches and have the capacity to self-renew or differentiate to form all blood cells throughout the lifespan of an animal[1–3]. Allogeneic HSC transplantation is a life-saving treatment for malignant and non-malignant disorders[4,5]. HSCs isolated from umbilical cord blood (CB) are used for hematopoietic cell transplantation (HCT)[6–11], but due to limited numbers of HSCs in single units of umbilical CB, a number of methods have been proposed for *ex vivo* expansion of human HSCs[7,8,12]. We show here that antagonism of the nuclear hormone receptor PPARγ promotes *ex vivo* expansion of phenotypically and functionally-defined subsets of human CB HSCs and hematopoietic progenitor cells (HSPCs). PPARγ antagonism in CB HSPCs strongly downregulated expression of several differentiation associated genes, as well as fructose 1, 6-bisphosphatase (*FBP1*), a negative regulator of glycolysis, and enhanced glycolysis without compromising mitochondrial metabolism. The expansion of CB HSPCs by PPARγ antagonism was completely suppressed by removal of glucose or inhibition of glycolysis. Moreover, knockdown of *FBP1* expression promoted glycolysis and *ex vivo* expansion of long-term repopulating CB HSPCs, whereas overexpression of *FBP1* suppressed the expansion of CB HSPCs induced by PPARγ antagonism. Our study suggests the possibility for a new and simple means for metabolic reprogramming of CB HSPCs to improve the efficacy of HCT.

Correspondence to: Hal E. Broxmeyer, Ph.D., hbroxmey@iupui.edu.
*These authors contributed equally to this work.

AUTHOR CONTRIBUTIONS

B.G. conceived the research, designed and performed experiments, interpreted data and wrote the manuscript. X.H. designed and performed Seahorse Extracellular Flux Assay, transplantation and interpreted data. M.R.L and S.A.L designed teratoma formation experiment and analyzed the results. H.E.B. supervised the study, designed and performed experiments, interpreted data and wrote the manuscript.

COMPETING FINANCIAL INTERESTS

Dr. Broxmeyer is a member of the Medical Scientific Advisory Board of Cord Use, a cord blood banking company based in Orlando, Florida.

Results and Discussion

The limited numbers of HSCs that are present in single units of CB is still an obstacle for more widespread clinical use of CB for HCT[7,8]. To overcome this limitation, a number of efforts to expand HSCs in CB have been made[10–16]. However, there is need for other means to improve the clinical efficacy of HCT through a better mechanistic understanding of the regulation and *ex vivo* expansion of CB HSPCs.

We first performed a compound screen to search for small molecules that could promote *ex vivo* expansion of a rigorously-defined flow-characterized population of HSCs (Lin$^-$CD34$^+$CD38$^-$CD45RA$^-$CD49f$^+$CD90$^+$)[17] isolated from fresh human CB, as tested in RPMI-1640 medium containing 10% fetal bovine serum (FBS) and cytokines (SCF, FL, TPO). From a nuclear hormone receptor ligand library comprising 74 compounds[18], we found that a PPARγ antagonist, GW9662, significantly enhanced cytokine stimulated (SCF, FL, TPO) *ex vivo* expansion of this population of human CB HSCs at days 4 and 7 of culture (Fig. 1a–c and Supplementary Fig. 1a,b and Supplementary Fig. 2a and Supplementary Table 1). GW9662 also enhanced expansion of CB CD34$^+$CD38$^-$ cells and multipotential progenitors (MPPs, Lin$^-$CD34$^+$CD38$^-$CD45RA$^-$CD49f$^-$CD90$^-$) (Supplementary Fig. 2b,c). Another PPARγ antagonist, T0070907, also enhanced expansion of human CB HSCs, whereas modulating the activity of PPARα or PPARδ had no effect on *ex vivo* expansion of CB HSCs (Supplementary Fig. 2d).

Hematopoietic progenitor cells (HPCs) also contribute to steady-state hematopoiesis during most of adulthood[19]. GW9662 significantly increased the numbers of CB colony-forming unit (CFU) granulocyte/macrophage (GM), and granulocyte, erythroid, macrophage, megakaryocyte (CFU-GEMM) progenitors after 4 days of *ex vivo* culture (Fig. 1d), demonstrating that antagonism of PPARγ also promotes *ex vivo* expansion of functionally recognizable HPCs.

PPARG (*PPARγ*) was highly expressed in CB HSCs and MPPs (Supplementary Fig. 2e,f). Notably, knockdown of *PPARγ* significantly enhanced *ex vivo* expansion of CB HSCs (Supplementary Fig. 2g,h), suggesting PPARγ signaling might function as a negative regulator of CB HSC self-renewal.

The effect of GW9662 on expansion of human CB HSCs was reversible (Supplementary Fig. 3a), and GW9662 by itself in the absence of cytokines had no mitogenic activity (Supplementary Fig. 3b). The rate of cell division and apoptosis were unchanged by GW9662 treatment (Supplementary Fig. 3c,d). In contrast to its effects on human CB HSCs, GW9662 did not promote *ex vivo* expansion of phenotypically-defined mouse HSCs (CD150$^+$CD48$^-$LSK) (Supplementary Fig. 4a,b).

To assess whether the *ex vivo* expansion of functional human CB HSPCs is enhanced by PPARγ antagonism, we transplanted progeny of 30,000 CB CD34$^+$ cells cultured with vehicle control or GW9662 for 4 days into sublethally irradiated NSG mice. Engraftment of CB CD34$^+$ cells in primary recipients was significantly increased in both BM and peripheral blood (PB) by treatment of the cultured cells with GW9662, as compared to vehicle control (Fig. 2a,b). Treatment with GW9662 also increased the percentages of both myeloid and

lymphoid lineage cells in the BM of primary recipients (Fig. 2c–e and Supplementary Fig. 5a–c), demonstrating that GW9662-cultured CB CD34$^+$ cells contain functionally engrafting HSCs. Next, we tested the effect of *PPARγ* knockdown by transplanting CB CD34$^+$ cells transfected with control shRNA or *PPARγ* shRNA into NSG recipient mice. As compared to control shRNA, transfection of CB CD34$^+$ cells with *PPARγ* shRNA enhanced both myeloid and lymphoid chimerism in the BM of recipients (Supplementary Fig. 5d). We confirmed the long-term reconstituting and self-renewing capability of GW9662-treated CB CD34$^+$ cells; 4 months after transplantation of BM from primary recipients into sublethally-irradiated secondary NSG recipient mice, myeloid and lymphoid chimerism in both the PB and BM were enhanced in the GW9662 treatment group, as compared to the vehicle treatment group (Fig. 2f and Supplementary Fig. 6a). We performed two independent limiting dilution experiments to calculate SCID-repopulating cells (SRC)[1], a measure of the number of functionally engrafting human HSCs. Cells cultured in cytokines (SCF, FL, TPO) did not demonstrate enhanced SRC numbers compared to uncultured CD34$^+$ cells, but the SRC frequency of GW9662-cultured CB CD34$^+$ cells was 4 fold higher than that of day 0 uncultured CD34$^+$ cells, and 5 fold higher than that of vehicle-treated CD34$^+$ cells cultured in cytokines (Fig. 2g,h and Supplementary Fig. 6b,c and Supplementary Tables 2,3,4,5). These data demonstrate that antagonism of PPARγ in CB CD34$^+$ cells leads to increased numbers of long-term engrafting and self-renewing HSCs.

To gain mechanistic insight into how PPARγ antagonism promotes *ex vivo* expansion of human CB HSPCs, we performed RNA sequencing (RNA-seq) analysis. Treatment of CB CD34$^+$ cells with GW9662 resulted in downregulation of a number of differentiation associated genes[20–25], including *CD38*, *CD1d*, *HIC1*, *FAM20C*, *DUSP4*, *DHRS3* and *ALDH1A2* (Fig. 3a,b and Supplementary Fig.7a,b), suggesting that PPARγ antagonism may maintain stemness of CB CD34$^+$ cells, at least in part by preventing differentiation. We also observed that *FBP1*, encoding fructose 1,6-bisphosphatase, a negative regulator of glycolytic flux[26,27], was significantly downregulated in GW9662-treated CB CD34$^+$ cells (Fig. 3a and Supplementary Fig.7a,b). We confirmed that FBP1 expression was decreased in GW9662 treated CB CD34$^+$ cells by real-time quantitative PCR, western blot and flow cytometry analysis (Fig. 3b–f). GW9662 treatment did not significantly change the expression of other genes involved in glycolysis of HSCs (*PKM2*, *LDHA*)[28] (Supplementary Fig. 7c), suggesting the specific targeting of PPARγ antagonism on *FBP1*. Since PPARδ-targeted fatty acid oxidation (FAO) regulates mouse HSC maintenance[29], we also checked the expression of genes involved in FAO. However, FAO-associated genes (*CPT1A*, *ANGPTL4*, *ACOX1*) were not increased by PPARγ antagonism in CB HSPCs (Supplementary Fig. 7d). Consistent with the data which shows no significant effect of GW9662 on mouse BM HSPC expansion, those differentiation associated genes and *Fbp1* in mouse BM HSPCs were not down-regulated by PPARγ antagonism (Supplementary Fig. 7e). We then wondered whether PPARγ antagonism would promote glycolysis. By directly measuring the extracellular acidification rate (ECAR) using a Seahorse XF Extracellular Flux instrument, we observed that GW9662-treated CB CD34$^+$ cells had significant higher glycolytic activity than that of vehicle-treated cells (Fig. 3g). Moreover, GW9662 treatment of CB CD34$^+$ cells promoted glucose uptake and lactate production (Fig. 3h,i). In contrast, the extracellular oxygen consumption rate (OCR) was not affected by GW9662 (Fig. 3j), suggesting that PPARγ

antagonism enhances glycolysis without compromising mitochondrial metabolism. *Ex vivo* expansion of CB HSCs by GW9662 was blocked by glucose depletion (Fig. 3k), as well as by administration of 2-deoxy-D-glucose (2-DG) (Fig. 3l), a well characterized inhibitor of glycolysis[30]. These data demonstrate that HSPC expansion by PPARγ antagonism depends on its enhancement of glucose metabolism.

To test whether loss of *FBP1* is sufficient to promote *ex vivo* expansion of human CB phenotypic HSCs (pHSCs), we treated CB $CD34^+$ cells with MB05032, a specific inhibitor of FBP1[31], or transfected cells with shRNA targeting *FBP1*. As compared to vehicle treatment, treatment with MB05032 significantly promoted expansion of human CB pHSCs and $CD34^+CD38^-$ cells (Fig. 4a and Supplementary Fig. 8a and Supplementary Fig. 9a and Supplementary Table 6); this expansion was dependent on continuous treatment with MB05032 (Supplementary Fig. 9b). Knockdown of *FBP1* also promoted expansion of CB pHSCs (Fig. 4b and Supplementary Fig. 9c). Although overexpression of *FBP1* had no effect on expansion of CB pHSCs, it completely blocked the expansion of CB pHSCs induced by PPARγ antagonism (Fig. 4c). Consistent with the concept that repression of *FBP1* plays a key role in the expansion of human CB pHSCs by PPARγ antagonism, *FBP1* overexpression significantly suppressed the increase in SRCs of GW9662-treated $CD34^+$ cells (Fig. 4d,e and Supplementary Table 7). MB05032 treatment also increased the numbers of CFU-GM, and CFU-GEMM progenitors (Supplementary Fig. 9d). MB05032 treatment did not further enhance the effects of GW9662 on expansion of CB pHSCs and CFUs (Supplementary Fig. 9e,f), indicating that PPARγ and FBP1 likely function in the same pathway.

Next, we performed a limiting dilution engraftment assay to determine the functional HSC frequency of CB $CD34^+$ cells cultured with cytokines and treated with either vehicle control or MB05032. MB05032-treated CB cells demonstrated significantly increased engraftment in primary NSG recipients 4 months after transplantation compared to the vehicle control group (Fig. 4f and Supplementary Fig. 9g,h), with increased human myeloid, B cell and T cell chimerism (Fig. 4f and Supplementary Fig. 9i–k). MB05032 treatment also significantly enhanced myeloid and lymphoid chimerism in secondary NSG mouse recipients (Supplementary Fig. 10a), suggesting that CB HSCs expanded by inhibition of FBP1 have long-term reconstituting capacity and self-renewal activity. Poisson distribution analysis revealed an SRC frequency of 1/4703 in uncultured day 0 CB $CD34^+$ cells, 1/5612 in vehicle-treated CB $CD34^+$ cells and 1/1328 in MB05032-treated CB $CD34^+$ cells (Fig. 4g,h and Supplementary Tables 4,5), suggesting the presence of 212 SRCs, 178 SRCs and 753 SRCs (3.6 fold increase) in 1×10^6 uncultured, vehicle– and MB05032-treateed cells, respectively. Another independent limiting dilution analysis showed a similar effect of MB05032 (Supplementary Fig. 10b,c and Supplementary Tables 8,9).

Since early recovery of myeloid cells is important in CB transplantation-based therapy, we also checked myeloid engraftment of GW9662 and MB05032 treated CB cells at 2 and 4 weeks after transplantation. Myeloid chimerism was significantly increased in both the PB and BM of recipients infused with GW9662– or MB05032-treated CB cells, as compared to vehicle-treated cells (Supplementary Fig. 10d–g).

Treatment with MB05032 promoted glycolysis, glucose uptake and lactate production of CB $CD34^+$ cells (Fig. 4i–k). Similarly to expansion of CB HSCs by PPARγ antagonism, expansion of CB HSCs by MB05032 was suppressed by depletion of glucose or by administration of 2-DG (Fig. 4l,m). This result is consistent with the concept that, by facilitating glycolysis, loss of *FBP1* promotes *ex vivo* expansion of human CB HSPCs. Due to the established role of FBP1 mediated glycolysis in cancer cells, we thus checked the safety of CB HSPCs expanded by antagonizing PPARγ-FBP1 axis. During our *in vivo* transplantation, we did not find any symptoms of leukemia. There was no significant change of the recipient survival rate between the control group and GW9662 or MB05032 treated group (Supplementary Fig. 11a,b). Also, we checked the histone acetylation and methylation levels in Vehicle, GW9662 or MB05032 treated CB HSCs, and did not find any significant change of the total levels of acH3K9, acH3K14, acH4K5, acH4K16 or tri-meH3K27 (Supplementary Fig. 11c–g), suggesting that the cell fate of GW9662 or MB05032-treated cells was not epigenetically reprogrammed. Consistently, we found that GW9662 or MB05032-treated CB $CD34^+$ cells did not induce teratoma formation *in vivo* (Supplementary Fig. 12). Taken together, antagonism of PPARγ-FBP1 signaling did not induce malignant transformation of CB HSPCs.

The mechanisms underlying self-renewal and expansion of human CB HSCs are poorly understood. In the present study, we performed a compound screen using an *ex vivo* expansion assay and found that the PPARγ antagonist GW9662 promoted the expansion of functionally engrafting HSCs from a phenotypically-defined population of HSCs ($Lin^-CD34^+CD38^-CD45RA^-CD49f^+CD90^+$)[17] in both primary and secondary transplantation assays. We also calculated SRCs in uncultured and *ex vivo* expanded $CD34^+$ cells by LDA analysis[1,32]. As has been seen in numerous other studies, the number of SRCs are much lower than the numbers of phenotypic HSC, consistent with the concept that not all phenotypically-defined HSCs have engrafting capability. Also, calculation of the number of SRCs is a relative quantitation of the number of functional human HSCs, not an absolute quantitation, as we cannot be sure that all potentially functional HSCs successfully engrafted the BM of recipient mice.

These results indicate that a PPARγ-FBP1 pathway acts to repress glycolysis and thereby restrict human CB HSC expansion. PPARs are members of the nuclear hormone receptor superfamily, a group of ligand-activated transcription factors involved in many physiological processes including differentiation, development, inflammation and metabolism[33–35]. Previous studies have identified certain nuclear receptors as key regulators of stemness and differentiation of embryonic stem cell and somatic stem cells[36]. Antagonism of the retinoic acid receptor (RAR) disrupts the reconstituting activity of mouse HSCs[37,38] but promotes the maintenance of human HSCs[39,40], suggesting that retinoid signaling plays different roles in mouse and human HSC fate determination. Considering that GW9662, and two other compounds, StemRegenin1 (SR1) and UM171, which have been shown to expand human CB HSPCs, have no effect on expansion of mouse HSCs[10,15], it may be that the self-renewal of mouse and human HSCs are differentially regulated.

Although a PML-PPARδ-FAO pathway has been reported to control asymmetric cell division of mouse HSCs[29], the function of PPAR signaling in human HSCs was not

previously described. Our findings demonstrate that antagonism of the PPARγ pathway drives expansion of human CB HSPCs by enhancing FBP1-repressed glycolysis and preventing differentiation. Use of either a PPARγ antagonist or FBP1 inhibitor enhances long-term engraftment of self-renewing human CB HSCs, thus suggesting a new strategy to facilitate human CB HSC expansion by driving glucose metabolism.

METHODS

Methods and associated references are available in the online version of the paper.

METHODS

Mice

NSG (NOD.Cg-Prkdc^{scid} IL2rg^{tm1Wjl}/SzJ; 6–8 weeks) mice were bred by the In Vivo Therapeutics Core of the Indiana University School of Medicine (IUSM), and maintained in the Laboratory Animal Resource Center (LARC) at IUSM. All animal experiments followed protocols approved by The Institutional Animal Care and Use Committee of IUSM.

Isolation of human CB CD34$^+$ cells and cell culture

Cord blood samples were obtained from CORD:USE Cord Blood Bank (Orlando, FL, USA). Mononuclear cells were isolated by density gradient centrifugation with Ficoll-Paque Plus (GE Healthcare, Piscataway, NJ, USA). CD34$^+$ cells were enriched with immunomagnetic selection kit (Miltenyi Biotec, Auburn, CA, USA) following the manufacturer's instructions. CB CD34$^+$ cells were cultured in RPMI-1640 medium (Lonza, 12-702Q) with 10% fetal bovine serum (GE Healthcare HyClone. SH30071.03), 100 ng/mL stem cell factor (SCF) (R&D Systems, #7466-SC-010/CF), thrombopoietin (TPO) (R&D Systems, #288-TP-200/CF), Fms-like tyrosine kinase 3 ligand (FL) (BioLegend, # 710802). For screening, 50, 000 CD34$^+$ cells were cultured in 24-wells plates for 4 days with the above medium in the presence of 1 μM compound from Nuclear Receptor Ligand Library (Enzo Life Sciences, Farmingdale, NY, USA). The following compounds were used: GW9662 (Tocris Bioscience, #1508), T0070907 (Selleck Chemicals, S2871), Rosiglitazone (Selleck Chemicals, S2556), GSK3787 (Selleck Chemicals, S8025), GW501516 (Tocris Bioscience, #5674), GW6471 (Tocris Bioscience, #4618), GW7647 (Tocris Bioscience, #1677), MB05032 (ApexBio, A3586). Dimethyl sulfoxide (DMSO) (Sigma, D2650) was used as vehicle control.

Isolation of mouse lineage negative bone marrow cells and cell culture

Mouse bone marrow lineage cell depletion was performed with the mouse lineage cell depletion kit according to the manufacturer's protocol (Miltenyi Biotec, Auburn, CA, USA). Lineage negative mouse bone marrow cells were cultured in RPMI-1640 medium (Lonza, 12-702Q) with 10% fetal bovine serum (GE Healthcare HyClone. SH30071.03), 100 ng/mL mouse stem cell factor (mSCF) (R&D Systems, #455-MC-010), 100 ng/mL mouse thrombopoietin (mTPO) (R&D Systems, # 488-TO-005/CF), 100 ng/mL mouse Fms-like tyrosine kinase 3 ligand (mFtl3L) (BioLegend, #550706).

Immunostaining and Flow cytometry

Immunostaining and flow cytometry analysis were performed as previously described[18,32]. Cells were collected by centrifuging at 300 g for 10 min, washed twice with cold PBS, and resuspended in 200 μL PBS. Cells were stained with fluorescence conjugated antibodies at 4°C for 30 min. Cells were washed with cold PBS and cell pellets were fixed with 1% formaldehyde. Samples were analyzed on an LSRII flow cytometer (BD Biosciences). For intracellular staining, after cell surface staining, cells were fixed and permeabilized using Cell Permeabilization Kit (Thermo Fisher, Florence, KY, USA). Cells were washed with cold PBS, and stained with primary antibodies at room temperature for 20 min. APC or FITC-conjugated secondary antibodies were added, and cells incubated for another 20 min. Cells were washed and fixed for flow cytometry analysis. The following antibodies from BD Bioscience (San Jose, CA, USA) were used for cell surface staining (1:200 dilution): CD34-APC (581), CD38-PE (HIT2), CD45RA-PE-CF594 (HI100), CD90-PEcy7 (5E10), CD49f-PerCPcy5.5 (GoH3), CD3-FITC (UCHT1), CD19-PE (HIB19), CD33-PEcy7 (WM53) and CD45-APC (HI30). The following antibodies were used for intracellular staining (1:200 dilution): anti-PPARγ [E-8] (Santa Cruz Biotechnology, Santa Cruz, CA, USA), anti-FBP1 [EPR4620] (Abcam, Cambridge, MA, USA), anti-H4K5ac (9672), and anti-H4K16ac (13534) (Cell Signaling Technology, Beverly, MA, USA) and anti-H3K9ac (06-942) and anti-H3K14ac (07-353) (Millipore, Kankakee, IL, USA), anti-Histone H3 (tri methyl K27, ab6002) antibody (Abcam, Cambridge, MA, USA). For mouse staining, the following antibodies were used (1:200 dilution): Brilliant Violet 421 anti-mouse Lineage cocktail (Biolegend, #133311), PE/Cy7 anti-mouse Ly-6A/E (Sca-1) (Biolegend, #122513), APC anti-mouse CD117 (c-Kit) (Biolegend, #105811), FITC anti-mouse CD48 (Biolegend, #103404), PerCP/Cy5.5 anti-mouse CD150 (Biolegend, #115922). For phenotypic HSC quantification in *ex vivo* expansion assays, $Lin^{-}CD34^{+}CD38^{-}CD45RA^{-}CD49f^{+}CD90^{+}$ human cord blood cells are defined as phenotypic HSC (pHSC). By flow analysis, we can determine the frequency of pHSC in cultures of cord blood $CD34^{+}$ cells. A total of 50,000 $CD34^{+}$ cells were cultured; the total number of $CD34^{+}$ cells were counted on days 4 and 7, and the frequency of pHSC was determined by flow cytometry at days 0, 4 and 7.

CFSE labeling assay

CB $CD34^{+}$ cells were labeled with CellTrace™ CFSE dye (Thermo Fisher Scientific, Waltham, MA, USA) following the manufacturer's instructions. $CD34^{+}$ cells were incubated with 5 μM CFSE for 20 min at 37 °C, and protected from light. Cells were washed with culture medium containing 1% BSA. Labeled cells were cultured for 24 hours. $CD34^{+}$ cells from a single CFSE peak were sorted using a FACSAria instrument (BD Biosciences). Sorted cells were cultured with expansion medium (SCF, TPO, FL) in the presence of vehicle or GW9662. Four days later, CFSE intensity of $CD34^{+}$ cells was analyzed by flow cytometry.

Annexin V staining

Vehicle or GW9662 treated $CD34^{+}$ cells were stained with human CD34-APC (581) antibody for 30 min on ice. After washing, cells were stained with FITC labeled-Annexin V

(BD Biosciences, #556419) for 15 min at room temperature, then washed and fixed. The percentage of apoptotic cells was determined by FACS.

Colony-forming unit assay

Human cord blood $CD34^+$ cells were plated in semi-solid methylcellulose culture medium in the presence of 30% fetal bovine serum (FBS) (GE Healthcare HyClone. SH30071.03), 2 mM L-glutamine (Lonza, 17-605E), 100 μM β-mercaptoethanol (Sigma, M6250), 1U/mL Erythropoietin (EPO) (R&D Systems, 287-TC-500), 50 ng/mL SCF (R&D Systems, #7466-SC-010/CF), 10 ng/mL IL-3 (R&D Systems, 203-IL-050/CF) and 10 ng/mL GM-CSF (R&D Systems, 7954-GM-010), and were cultured in a 5% O_2/5% CO_2 humidified incubator[32]. The number of colonies was scored 14 days after seeding with an inverted microscope.

In vivo transplantation

The progeny cells of 30,000 $CD34^+$ CB cells treated with vehicle or GW9662 for 4 days were intravenously transplanted into sublethally irradiated primary NSG recipient mice (350 cGy; ^{137}Cs source, single dose). The percentage of human $CD45^+$ cells in the peripheral blood was checked at 2 and 4 months after transplantation. Primary recipient mice were sacrificed and the percentage of human $CD45^+$, $CD33^+$, $CD19^+$ and $CD3^+$ cells in the bone marrow was checked by immuno-staining and flow cytometry. For second transplantation, 5×10^6 bone marrow cells from primary recipients were intravenously transplanted into sublethally irradiated secondary NSG recipient mice. The percentage of human $CD45^+$ $CD33^+$ and $CD19^+$ cells in peripheral blood or bone marrow was checked at 4 months after transplantation.

Limiting dilution analysis

The frequency of human SCID repopulating cells (SRCs) was determined by limiting dilution analysis (LDA) as previously reported[32]. Increasing doses of uncultured, vehicle, GW9662 or MB05032 treated $CD34^+$ cells (500, 2,500 or 10,000 cells) were intravenously injected into sublethally irradiated NSG recipient mice (350 cGy; ^{137}Cs source, single dose). Three or four months after transplantation, the percentage of human $CD45^+$ cell chimerism was analyzed by immuno-staining and flow cytometry. For long-term engraftment assay, 5×10^6 bone marrow cells from the primary recipients of the 10,000-cell group were intravenously transplanted into secondary recipient mice. Based on our immuno-staining and flow cytometry analysis, we found that negative control samples sometimes show 0.1~0.3 % human $CD45^+$ cells. In order to exclude non-specific staining, we defined samples with >1% human $CD45^+$ cells as indicative of successful transplantation[32]. The HSC frequency was calculated using L-Calc software (Stem Cell Technologies Inc, Vancouver, BC, Canada) and plotted using ELDA software (bioinf.wehi.edu.au/software/elda/).

RNA extraction and Real-time PCR

RNA was extracted using the RNeasy Mini Kit following manufacturer's protocol (QIAGEN, #74106). Total RNA was reverse transcribed using Invitrogen Superscript III kit. Quantitative real-time PCR reactions were performed using SYBR Green PCR Master Mix (Thermo Fisher, Florence, KY, USA) and an Agilent Mx3000P QPCR System. GAPDH was

used as an internal control. The data are shown as relative mRNA level normalized to the level in vehicle control, which was set to 1. *FBP1* primers were: sense primer: 5'-TCAAGTTAAGAAGCTGGACG-3', anti-sense primer: 5'-CTCAGAAGGCTCATCAGTTG-3'. *CD1d* primers were: sense primer: 5'-ATCTCGTCCTTCGCCAATAG-3', anti-sense primer: 5'-ATATATGCTGCAGCGTCTCC-3'. *DHRS3* primers were: sense primer: 5'-GCACTGAGTGCCATTACTTC-3', anti-sense primer: 5'-ATGTGGCCATTCTGCAGCTC-3'. *ALDH1A2* primers were: sense primer: 5'-AGAACAGGTGTGTGAAGTTC-3', anti-sense primer: 5'-AGCTTGCAGGAATGGTTTGC-3'. *HIC1* primers were: sense primer: 5'-GTGACAACCTGTACGTGTGC-3', anti-sense primer: 5'-CTTGTAGCTCTTGTCGCACG-3'. *CD38* primers were: sense primer: 5'-GTAGACTGCCAAAGTGTATG-3', anti-sense primer: 5'-TCAGCAAGGTAGCCTAGCAG-3'. *FAM20C* primers were: sense primer: 5'-TACTGCGAGGAGGTGAAGCA-3', anti-sense primer: 5'-AGAGCTCGTCGTGCGAATAC-3'. *DUSP4* primers were: sense primer: 5'-AGATGGACTGCAGTGTGCTC-3', anti-sense primer: 5'-GGTGTTACAGCGCACGTTGA-3'. *GAPDH* primers were: sense primer: 5'-TTCGTCATGGGTGTGAACCA-3', anti-sense primer: 5'-TGGCAGTGATGGCATGGACT-3'. *CPT1A* primers were: sense primer: 5'-GTATCTACAGTCGGTGAGGC-3', anti-sense primer: 5'-GGATATACAGCAGATCCATG-3'. *ANGPTL4* primers were: sense primer: 5'-CCTGCGAATTCAGCATCTGC-3', anti-sense primer: 5'-TTGAAGTCCACTGAGCCATC-3'. *ACOX1* primers were: sense primer: 5'-GAGGACTTGAACTTCCTCAC-3', anti-sense primer: 5'-TCCGCAGTTGCCTGGTGAAG-3'. *PKM2* primers were: sense primer: 5'-CCGCCTGGACATTGATTCAC-3', anti-sense primer: 5'-GTGTCTAGAGCCACAGCAAC-3'. *LDHA* primers were: sense primer: 5'-GCAGATGAACTTGCTCTTGT-3', anti-sense primer: 5'-ATGTTCACGTTACGCTGGAC-3'.

Western blotting

CB CD34$^+$ Cells were lysed in RIPA buffer (25 mM Tris-HCl pH 7.6, 150 mM NaCl, 1% sodium deoxycholate, 0.1% SDS) with Halt TM Protease Inhibitor Cocktail (Thermo Fisher, Florence, KY, USA) on ice for 30 min. Samples were centrifuged at 4 °C, 13, 000 g for 15 min. Supernatants were collected and protein concentrations of the supernatants were quantified by Protein Quantitation Kit (Abcam, Cambridge, MA, USA). Samples were subjected to SDS-PAGE analysis and signals were detected using corresponding primary and secondary antibodies. The following antibodies (Sigma Aldrich, St. Louis, MO, USA) were used (1:1000 dilution): anti-FBP1 (HPA005857) and anti-actin (A3853).

RNA sequencing

Vehicle or GW9662 treated CB CD34$^+$ cells were lysed and RNA was extracted using the RNeasy Mini Kit (QIAGEN, Valencia, CA, USA). RNA sequencing analysis was performed at SeqWright Genomic Services (GE Healthcare). Briefly, RNA samples were subjected to

poly-A selection, TruSeq RNA sample preparation, library construction, and cluster generation. RNA libraries were sequenced on an Illumina HiSeq 2500 instrument with 2×100 bp read lengths for a total of 2×20 M reads per sample.

Seahorse extracellular flux assay

The extracellular acidification rate (ECAR) or oxygen consumption rate (OCR) of human CB $CD34^+$ cells was determined using a Seahorse XF Extracellular Flux Analyzer (Agilent Technologies). 200 μL XF Calibrant buffer (Seahorse Bioscience, #100840-000) was added into the wells of a Seahorse Bioscience 96-well utility plate, and then the plate was incubated at 37°C overnight. The cell culture plate (Seahorse Bioscience, # 101085-004) was coated with Cell-Tak solution (CORNING, # 354241) at room temperature for one hour. *Ex vivo* expanded CB $CD34^+$ cells were purified using human CD34 MicroBead Kit (Miltenyi Biotec, San Diego, CA 92121 USA), cells were resuspended with assay medium, and cell number was determined using a hemacytometer. 100,000 purified $CD34^+$ cells per well were plated into cell culture plates. The plates were centrifuged for 10 min, at 1,000 g. Glucose (Sigma, G8644), oligomycin (Sigma, #75351), 2-DG (Sigma, D8375) medium or oligomycin, FCCP (Sigma, C2920), rotenone (Sigma, R8875) medium was sequentially added into the wells of a utility plate for ECAR or OCR analysis. The utility plate with the loaded sensor cartridge was placed on the instrument tray for calibration. When prompted, replace the calibration plate with the cell culture microplate then click “Start” to evaluate ECAR or OCR of CB $CD34^+$ cells.

Knockdown and overexpression assay

For *PPARγ* or *FBP1* knockdown, shRNA expression plasmids (psi-LVRU6GP, obtained from Genecopeia) targeting *PPARγ* (5’-TCTTCCGGAGAACAATCAG-3’) or *FBP1* (5’-TGCACCTTACATTCCTAGA-3’) were transfected into CB $CD34^+$ cells by nucleofection (Amaxa™ Nucleofector™ Technology) following Lonza's optimized protocols (Lonza, VPA-1003). For overexpression of *FBP1*, human *FBP1* cDNA was cloned into pEGFP-N1 (Clontech), and the empty vector control or pEGFP-N1-FBP1 were transfected into CB $CD34^+$ cells using nucleofector.

Glucose uptake assay

Glucose uptake analysis was performed using the 2-NBDG Glucose Uptake Assay Kit (BioVision, Milpitas, CA, USA) following the manufacturer’s protocol. CB $CD34^+$ cells were cultured in expansion medium with 0.5% FBS in the presence of vehicle, GW9662 or MB05032 for 4 days. Cells were incubated with glucose uptake mix at 37 °C with 5% CO_2 for 30 min. After incubation, cells were collected from the plate and kept on ice. Cells were washed once with ice-cold analysis buffer and resuspended in analysis buffer and then analyzed by FACS.

Lactate secretion assay

CB $CD34^+$ cells were cultured in expansion medium with 10% dialyzed FBS in the presence of vehicle GW9662 or MB05032 for 4 days. The relative lactate level in the medium was analyzed using the Lactate Colorimetric/Fluorometric Assay Kit (BioVision, Milpitas, CA,

USA). 10 μL sample was added into 40 μL Lactate Assay Buffer, and then 50 μL Reaction Mix was added into each diluted sample. The reaction was incubated for 30 min at room temperature, protected from light. Absorbance at OD570 nm was measured in a microplate reader. All assays were performed in triplicate.

Teratoma formation analysis

1×10^6 vehicle, GW9662, MB05032-treated $CD34^+$ cells or 1×10^6 human H9 ES cells were injected into the testis of NOD SCID mice, and teratomas were examined after 8 weeks[32]. Samples from the teratomas were paraffin embedded and serially sectioned using a microtome (Leica Microsystems, Wetzlar, Germany). To analyze three germ-layer lineage cells in teratomas derived from injected H9 ES cells which served as a positive control, sectioned slides were stained. The tissues representing all 3 embryonic germ layers, including secretory epithelium (PAS stain), cartilage (Alcian blue stain), and gut epithelium (H & E stain), were examined. Images were analyzed using an inverted microscope system (Nikon, Tokyo, Japan).

Statistical analysis

Statistical analysis was performed using Microsoft Excel and GraphPad Prism 5.0. Data are shown as mean values ± standard deviation (SD), unless stated otherwise as standard error of the mean (SEM). Two-tailed Student's *t*-tests were performed for statistical analysis between two groups. One-way analysis of variance (ANOVA) was used to compare differences in means between more than two groups where indicated. *P*-value less than 0.05 was considered as statistically significant.

Data availability

RNA-seq raw data are available in the Gene Expression Omnibus (GEO) database: Series GSE95703. Additional detailed information on experimental design and reagents for this study is provided in the **Life Sciences Reporting Summary**.

Supplementary Material

Refer to Web version on PubMed Central for supplementary material.

Acknowledgments

This work was supported by US Public Health Service Grants from the NIH to HEB: (R01 HL112669, R01 HL056416, U54 DK106846); and the National Research Foundation funded by the Korea government (NRF-2017M3A9C6033069). We thank Steven Messina-Graham for technical support during Seahorse assay, and other members in the Broxmeyer laboratory for helpful discussion and assistance, and Anthony L. Sinn from the In Vivo Therapeutics Core of the Indiana University School of Medicine for transplantation assistance.

References

1. Doulatov S, Notta F, Laurenti E, Dick JE. Hematopoiesis: A Human Perspective. Cell Stem Cell. 2012; 10:120–135. [PubMed: 22305562]
2. Morrison SJ, Scadden DT. The bone marrow niche for haematopoietic stem cells. Nature. 2014; 505:327–334. [PubMed: 24429631]

3. Eaves CJ. Hematopoietic stem cells: concepts, definitions, and the new reality. Blood. 2015; 125:2605–2613. [PubMed: 25762175]
4. Edward A, Copelan MD. Hematopoietic Stem-Cell Transplantation. N. Engl. J. Med. 2006; 354:1813–1826. [PubMed: 16641398]
5. Singh AK, McGuirk JP. Allogeneic Stem Cell Transplantation: A Historical and Scientific Overview. Cancer Res. 2016; 76:6445–6551. [PubMed: 27784742]
6. Broxmeyer HE, et al. Human umbilical cord blood as a potential source of transplantable hematopoietic stem/progenitor cells. Proc. Natl. Acad. Sci. USA. 1989; 86:3828–3832. [PubMed: 2566997]
7. Ballen KK, Gluckman E, Broxmeyer HE. Umbilical cord blood transplantation: the first 25 years and beyond. Blood. 2013; 122:491–498. [PubMed: 23673863]
8. Broxmeyer HE, Farag S. Background and future considerations for human cord blood hematopoietic cell transplantation, including economic concerns. Stem Cells Dev. 2013; 22:103–110. [PubMed: 24304086]
9. Milano F, et al. Cord-Blood Transplantation in Patients with Minimal Residual Disease. N. Engl. J. Med. 2016; 375:944–953. [PubMed: 27602666]
10. Fares I, et al. Pyrimidoindole derivatives are agonists of human hematopoietic stem cell self-renewal. Science. 2014; 345:1509–1512. [PubMed: 25237102]
11. Wagner JE, et al. Phase I/II Trial of StemRegenin-1 Expanded Umbilical Cord Blood Hematopoietic Stem Cells Supports Testing as a Stand-Alone Graft. Cell Stem Cell. 2016; 18:144–155. [PubMed: 26669897]
12. Nikiforow S, Ritz J. Dramatic Expansion of HSCs: New Possibilities for HSC Transplants? Cell Stem Cell. 2016; 18:10–12. [PubMed: 26748750]
13. Mantel CR, et al. Enhancing Hematopoietic Stem Cell Transplantation Efficacy by Mitigating Oxygen Shock. Cell. 2015; 161:1553–1565. [PubMed: 26073944]
14. Csaszar E, et al. Rapid expansion of human hematopoietic stem cells by automated control of inhibitory feedback signaling. Cell Stem Cell. 2012; 10:218–229. [PubMed: 22305571]
15. Boitano AE, et al. Aryl hydrocarbon receptor antagonists promote the expansion of human hematopoietic stem cells. Science. 2010; 329:1345–1348. [PubMed: 20688981]
16. Chaurasia P, Gajzer DC, Schaniel C, D'Souza S, Hoffman R. Epigenetic reprogramming induces the expansion of cord blood stem cells. J. Clin. Invest. 2014; 124:2378–2395. [PubMed: 24762436]
17. Notta F, et al. Isolation of single human hematopoietic stem cells capable of long-term multilineage engraftment. Science. 2011; 333:218–221. [PubMed: 21737740]
18. Guo B, Huang X, Cooper S, Broxmeyer HE. Glucocorticoid hormone-induced chromatin remodeling enhances human hematopoietic stem cell homing and engraftment. Nat. Med. 2017; 23:424–428. [PubMed: 28263313]
19. Sun J, et al. Clonal dynamics of native haematopoiesis. Nature. 2014; 514:322–327. [PubMed: 25296256]
20. Shubinsky G, Schlesinger M. The CD38 lymphocyte differentiation marker: new insight into its ectoenzymatic activity and its role as a signal transducer. Immunity. 1997; 7:315–324. [PubMed: 9324352]
21. Wei DG, et al. Expansion and long-range differentiation of the NKT cell lineage in mice expressing CD1d exclusively on cortical thymocytes. J. Exp. Med. 2005; 202:239–248. [PubMed: 16027237]
22. Lee JH, et al. Progesterone promotes differentiation of human cord blood fetal T cells into T regulatory cells but suppresses their differentiation into Th17 cells. J. Immunol. 2011; 187:1778–1787. [PubMed: 21768398]
23. Wang X, et al. Inactivation of a novel FGF23 regulator, FAM20C, leads to hypophosphatemic rickets in mice. PLoS. Genet. 2012; 8:e1002708. [PubMed: 22615579]
24. Su H, et al. PRMT1-Mediated Methylation of DUSP4 Determines Megakaryocyte-Erythroid Lineage Choice By Regulating p38 Signaling. Blood. 2015; 126:2387.

25. Rönn RE, et al. Retinoic Acid Regulates Hematopoietic Development from Human Pluripotent Stem Cells. Stem Cell Reports. 2015; 4:269–281. [PubMed: 25680478]
26. Dong C, et al. Loss of FBP1 by Snail-mediated repression provides metabolic advantages in basal-like breast cancer. Cancer Cell. 2013; 23:316–331. [PubMed: 23453623]
27. Li B, et al. Fructose-1,6-bisphosphatase opposes renal carcinoma progression. Nature. 2014; 513:251–255. [PubMed: 25043030]
28. Wang YH, et al. Cell-state-specific metabolic dependency in hematopoiesis and leukemogenesis. Cell. 2014; 158:1309–1323. [PubMed: 25215489]
29. Ito K, et al. A PML–PPAR-δ pathway for fatty acid oxidation regulates hematopoietic stem cell maintenance. Nat. Med. 2012; 18:1350–1358. [PubMed: 22902876]
30. Brown J. Effects of 2-deoxyglucose on carbohydrate metabolism: review of the literature and studies in the rat. Metabolism. 1962; 11:1098–1112. [PubMed: 13873661]
31. Erion MD, et al. MB06322 (CS-917): A potent and selective inhibitor of fructose 1,6-bisphosphatase for controlling gluconeogenesis in type 2 diabetes. Proc. Natl. Acad. Sci. USA. 2005; 102:7970–7975. [PubMed: 15911772]
32. Huang X, et al. Activation of OCT4 enhances *ex vivo* expansion of human cord blood hematopoietic stem and progenitor cells by regulating HOXB4 expression. Leukemia. 2016; 30:144–153. [PubMed: 26202933]
33. Yang XO, et al. T helper 17 lineage differentiation is programmed by orphan nuclear receptors ROR alpha and ROR gamma. Immunity. 2008; 28:29–39. [PubMed: 18164222]
34. Wu L, et al. Inhibition of PPARγ in myeloid-lineage cells induces systemic inflammation, immunosuppression, and tumorigenesis. Blood. 2012; 119:115–126. [PubMed: 22053106]
35. Evans RM, Mangelsdorf DJ. Nuclear Receptors, RXR, and the Big Bang. Cell. 2014; 157:255–266. [PubMed: 24679540]
36. Jeong Y, Mangelsdorf DJ. Nuclear receptor regulation of stemness and stem cell differentiation. Exp. Mol. Med. 2009; 41:525–537. [PubMed: 19696553]
37. Purton LE, Bernstein ID, Collins SJ. All-trans retinoic acid enhances the long-term repopulating activity of cultured hematopoietic stem cells. Blood. 2000; 95:470–477. [PubMed: 10627451]
38. Purton LE, et al. RARgamma is critical for maintaining a balance between hematopoietic stem cell self-renewal and differentiation. J. Exp. Med. 2006; 203:1283–1293. [PubMed: 16682494]
39. Chute JP, et al. Inhibition of aldehyde dehydrogenase and retinoid signaling induces the expansion of human hematopoietic stem cells. Proc. Natl. Acad. Sci. USA. 2006; 103:11707–11712. [PubMed: 16857736]
40. Ghiaur G, et al. Regulation of human hematopoietic stem cell self-renewal by the microenvironment's control of retinoic acid signaling. Proc. Natl. Acad. Sci. USA. 2013; 110:16121–16126. [PubMed: 24043786]

Editorial summary

A small molecule antagonist of PPARγ expands human CB HSPCs via downregulation of genes involved in cell differentiation and glycolysis, thereby preventing differentiation and enhancing glucose metabolism.

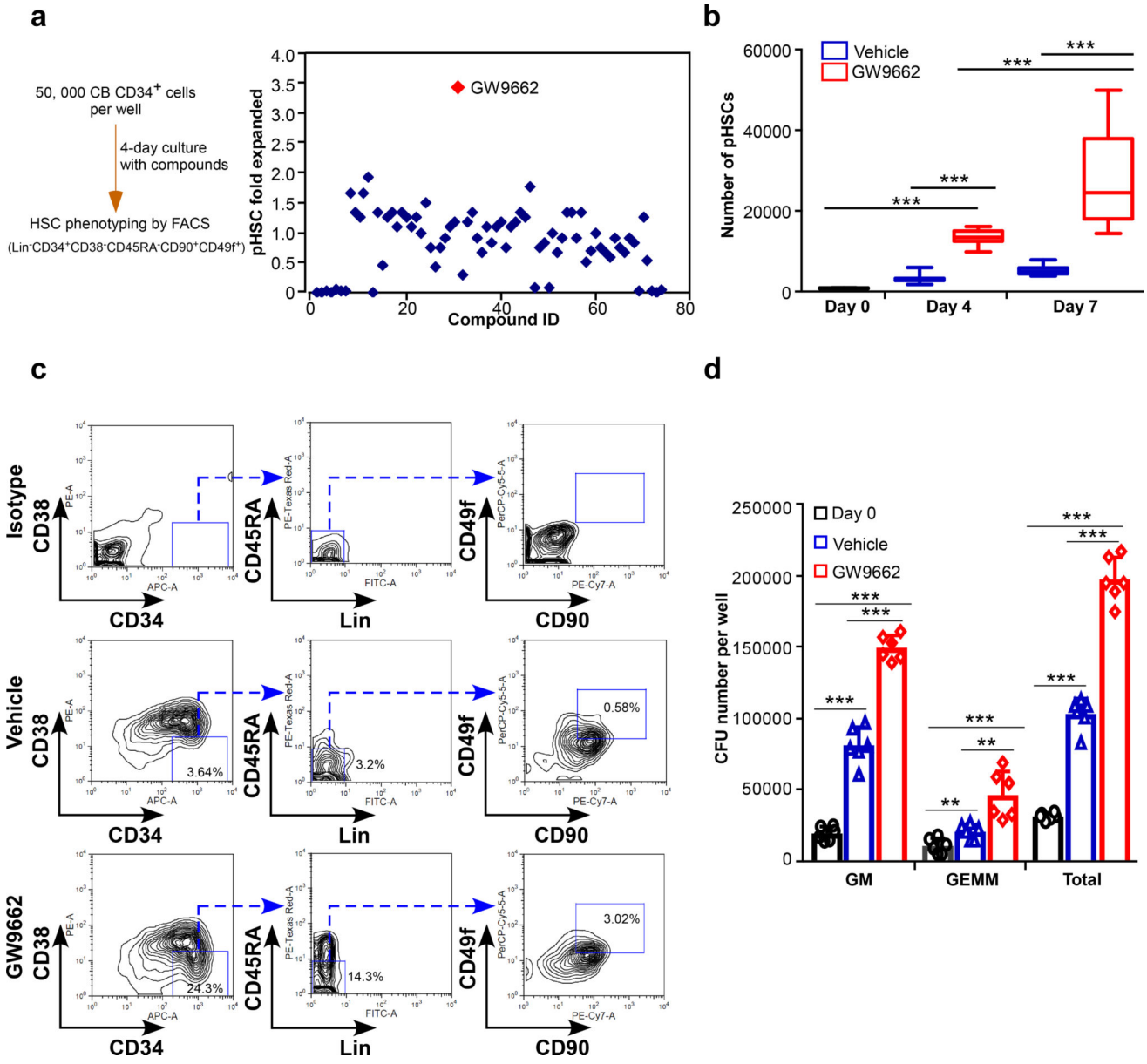

Figure 1. PPARγ antagonism promotes *ex vivo* expansion of human CB HSPCs

(**a**) Left, the experimental strategy for the compound screen used to identify GW9662, a PPARγ antagonist, as promoting CB HSC *ex vivo* expansion. Freshly isolated CB $CD34^+$ cells were cultured with vehicle control or compounds from the library for 4 days. Phenotypic HSC (pHSCs, $Lin^-CD34^+CD38^-CD45RA^-CD49f^+CD90^+$) expansion was determined by FACS analysis. Right, fold *ex vivo* expansion of CB pHSCs for the compounds tested. The red diamond indicates GW9662.

(**b**) Quantification data of CB pHSC *ex vivo* expansion by vehicle or GW9662 at days 4 and 7. 50,000 $CD34^+$ cells per well were plated at day 0 and the pHSC frequency was determined by flow cytometry. Data pooled from four independent experiments (n=12 cultures per group) are shown as box-and-whisker plots (the lines indicate median values, the whiskers indicate minimum and maximum values, the boxes indicate interquartile

range). The exact cell numbers from each experiment are shown in Supplementary Table 1. One-way ANOVA; ***p<0.001.

(**c**) Representative FACS plots showing expansion of CB pHSCs by GW9662. The pHSC population was assessed as $Lin^{-}CD34^{+}CD38^{-}CD45RA^{-}CD49f^{+}CD90^{+}$ cells in day 4 cultures. Gating was based on use of isotype control antibodies. The percentages indicate the frequencies of gated cell populations among the live cell events collected. Representative plots from 4 independent experiments are shown.

(**d**) CFU numbers in 50,000 cells of day 0 uncultured $CD34^{+}$ cells and the progeny of an equivalent number of $CD34^{+}$ cells that were expanded in the presence of vehicle control or GW9662 for 4 days (n=6 cultures from two independent experiments per group). One-way ANOVA; **p<0.01, ***P<0.001.

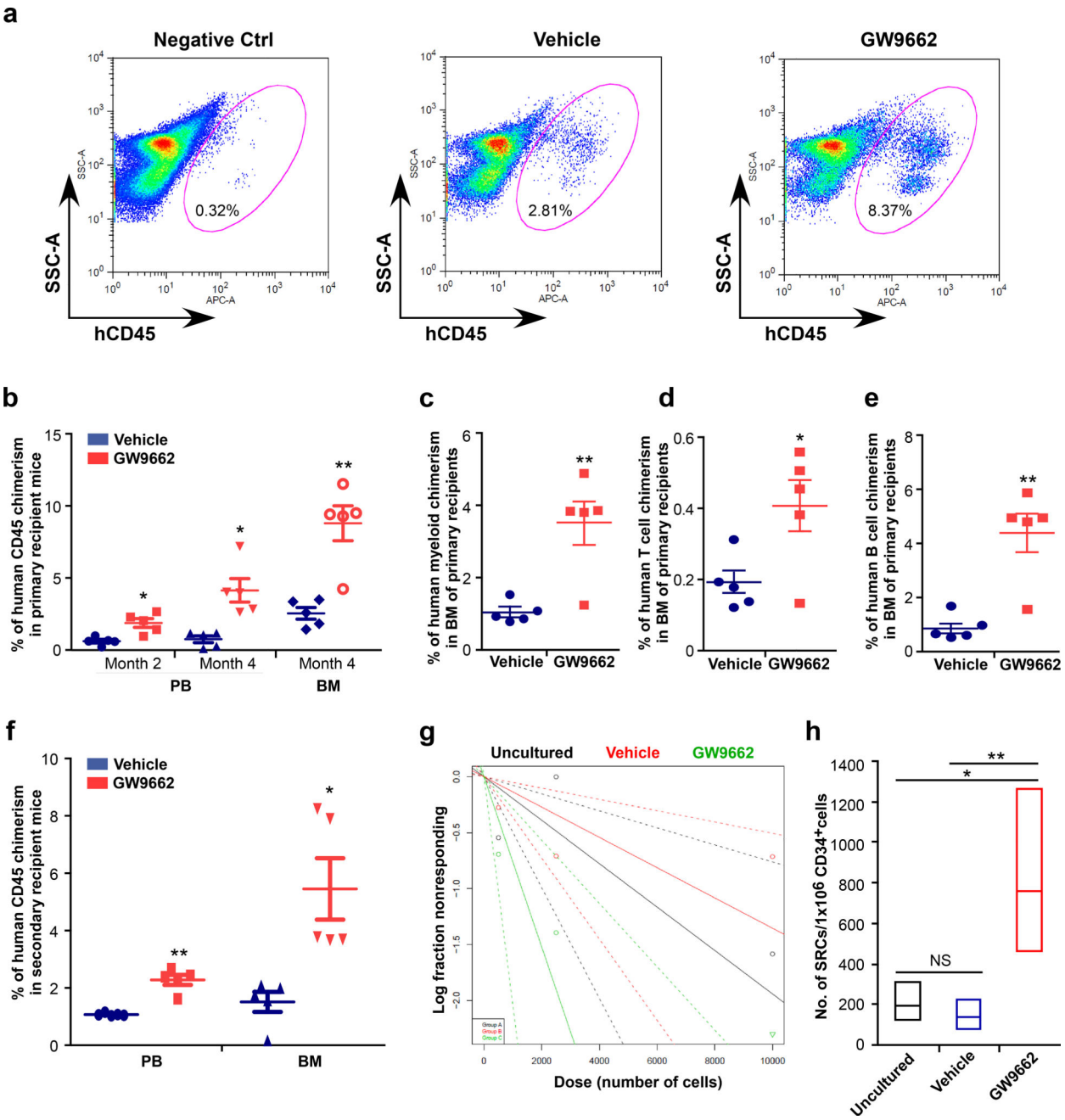

Figure 2. PPARγ antagonism expands long term HSCs from human cord blood

(**a**) Representative FACS plots showing the percent engraftment of vehicle control- or GW9662-treated human CB CD34$^+$ cells in the bone marrow of recipient NSG mice 4 months after transplantation. Non-transplanted mouse bone marrow cells were used as the negative control. Representative plots from 3 independent experiments are shown.

(**b**) The percentage of human CD45$^+$ cells in peripheral blood (PB) at 2 and 4 months, and the percentage of human CD45$^+$ cells in bone marrow (BM) at 4 months, after transplantation of NSG mice with the progeny of 30,000 CB CD34$^+$ cells treated with

vehicle or GW9662 for 4 days (n=5 mice per group). Data are shown as dot plots (mean ±s.e.m.). *p<0.05, **p=0.009.

(**c–e**) Human $CD33^+$ myeloid cell, $CD3^+$ T cell and $CD19^+$ B cell chimerism in the bone marrow (BM) of primary recipients at 4 months after transplantation (n=5 mice per group). Data are shown as dot plots (mean±s.e.m.). *p=0.032, **p<0.01.

(**f**) The engraftment of human $CD45^+$ cells in the peripheral blood and bone marrow of secondary recipient NSG mice at 4 months after transplantation (n=5 mice per group). Data are shown as dot plots (mean±s.e.m.). From (**b**) to (**f**), two-tailed Student's *t*-test was used. *p=0.017, **p=0.002.

(**g,h**) The frequency of human SRCs in uncultured CB $CD34^+$ cells or in the progeny of an equivalent number of $CD34^+$ cells treated by vehicle or GW9662 for 4 days. Graded doses of uncultured, vehicle or GW9662 treated CB $CD34^+$ cells were transplanted into irradiated NSG mice and the percentage of human $CD45^+$ cells in bone marrow (BM) was analyzed at 3 months after transplantation (n=2–5 mice per group, see Supplementary Table 2). Poisson statistical analysis of data from Supplementary Table 2 and 3 is shown in (**g**). The percentage of negative mice for each dose of cells is plotted. Inverted triangles indicate that all tested mice were positive in this group. Solid lines indicate the best-fit linear model for each data set. Group A (black line) corresponds to the uncultured group, group B (red line) corresponds to the vehicle-treated group, and group C (green line) corresponds to the GW9662-treated group. Dotted lines represent 95% confidence intervals. HSC frequencies (line in the box) and 95% confidence intervals (box) presented as the number of SRCs in 1×10^6 $CD34^+$ cells are shown in (**h**). NS, not significant; *p=0.0375, **p=0.00828. Results from another independent experiment are shown in Supplementary Figure 6b,c and Supplementary Tables 4 and 5.

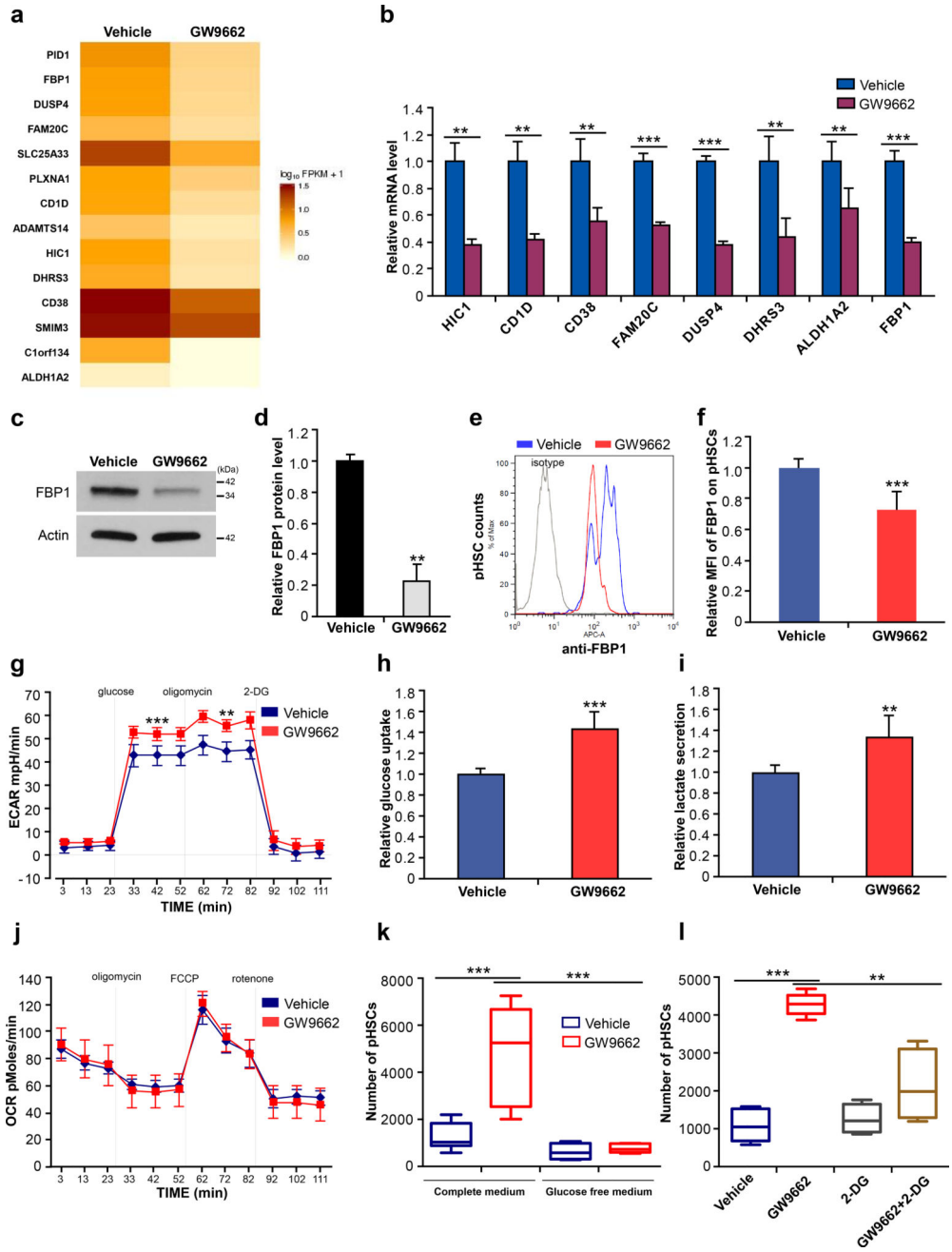

Figure 3. PPARγ antagonism promotes *ex vivo* expansion of human CB HSCs by switching on FBP1-repressed glycolysis

(**a**) Heat map showing gene expression downregulated by 4 days -GW9662 treatment of CB CD34$^+$ cells as compared to vehicle treatment.

(**b**) Relative mRNA level of targeted genes downregulated by GW9662 was determined by quantitative real-time PCR (n=6 replicates from two independent experiments). Two-tailed Student's *t*-test was used. **p<0.01, ***p<0.001.

(**c,d**) Western blot analysis of FBP1 expression in vehicle or GW9662 treated human CB CD34$^+$ cells. Representative blot and quantification data from three independent

experiments (n=3 independent experiments) are shown in (**c**) and (**d**). Actin was used as a loading control. Two-tailed Student's *t*-test was used. **p=0.004. The uncropped blot was shown in Supplementary Fig. 13.

(**e,f**) FBP1 expression in vehicle or GW9662 treated human CB HSCs, as analyzed by FACS. Representative histogram and quantification data from three independent experiments (n=3 independent experiments) are shown in (**e**) and (**f**). Two-tailed Student's *t*-test was used. ***p=0.0002.

(**g**) ECAR measurements in purified CB $CD34^+$ cells following a 4-day culture with vehicle or GW9662. Data pooled from three independent experiments are shown as mean±s.d. (n=3 independent experiments). Two-tailed Student's *t*-test was used. **p=0.0018, ***p=0.0008.

(**h**) Relative glucose uptake in vehicle or GW9662 treated CB $CD34^+$ cells. Glucose uptake was determined by FACS based on the mean fluorescence intensity (MFI) of the incorporated fluorescent glucose analog 2-NBDG (n=3 independent experiments). The value of vehicle group was set as "1". ***p=0.00016.

(**i**) Relative levels of lactate secreted by vehicle or GW9662 treated CB $CD34^+$ cells (n=3 independent experiments). **p=0.0049.

(**j**) OCR measurements in purified CB $CD34^+$ cells following a 4-day culture with vehicle or GW9662. Representative data from three independent experiments is shown as mean±s.d..

(**k**) CB HSC *ex vivo* expansion by vehicle or GW9662 in complete medium (with glucose) and glucose free medium. 50,000 $CD34^+$ cells per well were cultured in the indicated culture medium containing 10% dialyzed serum, and the number of pHSCs was determined at day 4. Data pooled from three independent experiments are shown as box-and-whisker plots (the lines indicate median values, the whiskers indicate minimum and maximum values, the boxes indicate interquartile range) (n=9 cultures per group). One-way ANOVA; ***p<0.001.

(**l**) CB HSC expansion in the presence of vehicle, GW9662, 2-DG (1 mM) or GW9662+2-DG (1 mM). 50,000 $CD34^+$ cells per well were cultured in the indicated conditions, and the number of pHSCs was determined at day 4. Data pooled from two independent experiments are shown as box-and-whisker plots (the lines indicate median values, the whiskers indicate minimum and maximum values, the boxes indicate interquartile range) (n=6 cultures per group). One-way ANOVA; **p=0.002, ***p<0.001.

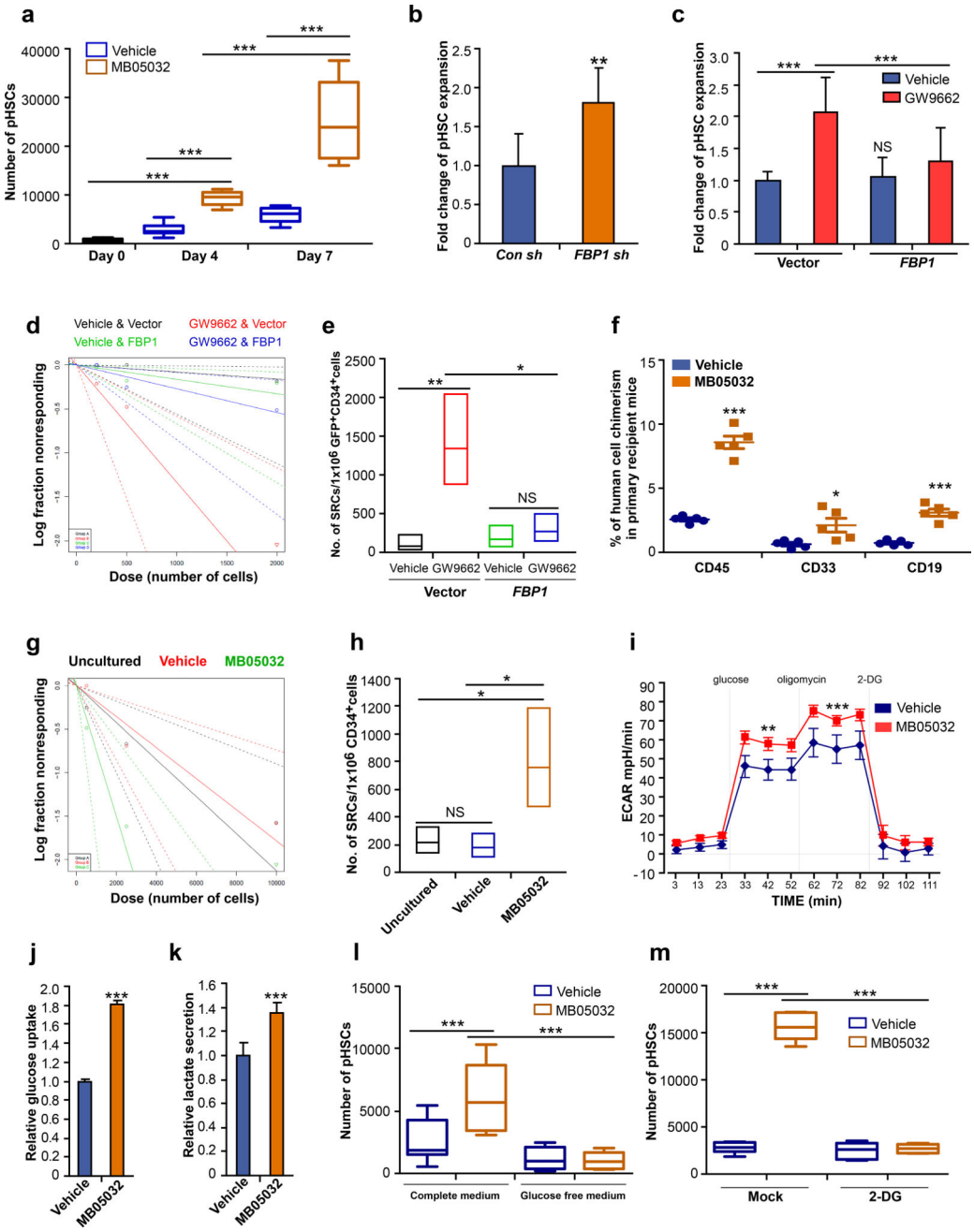

Figure 4. Loss of function of FBP1 expands CB HSPCs by enhancing glycolysis

(**a**) Quantification of CB HSC *ex vivo* expansion by vehicle or MB05032 at days 4 and 7. 50,000 $CD34^+$ cells per well were cultured and the phenotypic HSC frequency was determined at days 4 and 7. Data pooled from four independent experiments are shown as box-and-whisker plots (n=12 cultures per group). The exact cell numbers from each experiment are shown in Supplementary Table 6. One-way ANOVA; ***p<0.001. (**b**) Expansion of CB HSPCs transduced with scrambled control shRNA or *FBP1* shRNA and cultured for 4 days, as determined by FACS. Data pooled from two independent

experiments are shown (n=6 cultures per group). Two-tailed Student's *t*-test was used. **p=0.0015.

(**c**) Expansion of CB HSPCs transduced with control vector (pEGFP-N1) or pEGFP-N1-FBP1 and then cultured in expansion medium containing vehicle or GW9662 for 4 days, as determined by FACS (n=3 independent experiments). One-way ANOVA; NS, not significant; **p<0.01.

(**d,e**) The frequency of human SRCs in control vector or *FBP1* transfected CB $CD34^+$ cells treated with vehicle or GW9662. Graded doses of GFP^+CD34^+ cells were transplanted into irradiated NSG mice. The percentage of human $CD45^+$ cells in bone marrow (BM) was analyzed 2 months after transplantation (n=4–5 mice per group, see Supplementary Table 7). Poisson statistical analysis of data from Supplementary Table 7 is shown in (**d**). The percentage of negative mice for each dose of cells is plotted. Inverted triangles indicate that all tested mice were positive in this group. Solid lines indicate the best-fit linear model for each data set. Group A (black line) corresponds to the vehicle & vector group, and group B (red line) corresponds to the GW9662 & vector group, and group C (green line) corresponds to the vehicle & FBP1 group, group D (blue line) corresponds to the GW9662 & FBP1 group. Dotted lines represent 95% confidence intervals. HSC frequencies (line in the box) and 95% confidence intervals (box) presented as the number of SRCs in 1×10^6 GFP^+CD34^+ cells are shown in (**e**). NS, not significant; *p=0.021, **p=0.001.

(**f**) Human $CD45^+$ cell chimerism, human $CD33^+$ myeloid cell chimerism and human $CD19^+$ B cell chimerism in bone marrow (BM) of NSG mice at 4 months after transplantation of the progeny of 10,000 CB $CD34^+$ cells treated with vehicle or MB05032 for 4 days (n=5 mice per group). Another independent experiment is shown in Supplementary Fig. 9h–k. Data are shown as dot plots (mean±s.e.m.). Two-tailed Student's *t*-test was used. *p<0.05, ***p<0.001.

(**g,h**) The frequency of human SRCs in uncultured CB $CD34^+$ cells, and the progeny of an equivalent number of $CD34^+$ cells treated by vehicle or MB05032. Graded doses of uncultured, vehicle or MB05032 treated CB $CD34^+$ cells were transplanted into irradiated NSG mice. The percentage of human $CD45^+$ cells in bone marrow (BM) was analyzed 4 months after transplantation (n=4–5 mice per group, see Supplementary Table 4). Poisson statistical analysis of data from Supplementary Tables 4 and 5 is shown in (**g**). The percentage of negative mice for each dose of cells is plotted. Inverted triangles indicate that all tested mice were positive in this group. Solid lines indicate the best-fit linear model for each data set. Group A (black line) corresponds to the uncultured group, and group B (red line) corresponds to the vehicle-treated group, and group C (green line) corresponds to the MB05032-treated group. Dotted lines represent 95% confidence intervals. HSC frequencies (line in the box) and 95% confidence intervals (box) presented as the number of SRCs in 1×10^6 $CD34^+$ cells are shown in (**h**). NS, not significant; *p<0.05. Data from another independent experiment is shown in Supplementary Figure 10b,c and Supplementary Tables 8 and 9.

(**i**) ECAR measurements in purified CB $CD34^+$ cells following a 4-day culture with vehicle or MB05032. Data pooled from three independent experiments are shown as mean±s.d. (n=3 independent experiments). Two-tailed Student's *t*-test was used. **p<0.01; ***p<0.001.

(**j**) Relative glucose uptake in vehicle or MB05032 treated CB $CD34^+$ cells. Glucose uptake was determined by FACS based on the mean fluorescence intensity (MFI) of the

incorporated fluorescent glucose analog 2-NBDG (n=3 independent experiments). The value of vehicle group was set as "1". Two-tailed Student's *t*-test was used. ***p<0.001.
(**k**) Relative levels of lactate secreted by vehicle or MB05032 treated CB $CD34^+$ cells (n=3 independent experiments). Two-tailed Student's *t*-test was used. ***p<0.001.
(**l**) CB HSC *ex vivo* expansion by vehicle or MB05032 in complete medium (with glucose) and glucose free medium. 50,000 $CD34^+$ cells per well were plated in the indicated culture medium containing 10% dialyzed serum, and the phenotypic HSC frequency was determined by flow cytometry at day 4. Data pooled from three independent experiments are shown as box-and-whisker plots (n=9 cultures per group). One-way ANOVA; ***p<0.001.
(**m**) CB HSC expansion in the presence of vehicle, MB05032, 2-DG (1 mM) or MB05032+2-DG (1 mM). 50,000 $CD34^+$ cells per well were cultured in the indicated conditions, and the number of pHSCs was determined at day 4. Data pooled from two independent experiments are shown as box-and-whisker plots (n=6 cultures per group). For box-and-whisker plots in (**a**), (**l**) and (**m**), the lines indicate median values; the whiskers indicate minimum and maximum values; the boxes indicate interquartile range. One-way ANOVA; ***p<0.001.